Highly Pathogenic Avian Influenza A(H5N8) Clade 2.3.4.4b Viruses in Satellite-Tracked Wild Ducks, Ningxia, China, 2020

Appendix

Materials and Methods

Samples and Virus Isolation

A total of 275 paired oropharyngeal and cloacal swab specimens were collected from net-caught wild ducks at Changshantou Reservoir, Ningxia, western China (N37°16′14″, E105°43′5″), in October 2020. The samples were oscillated and then centrifuged, and the collected supernatant was inoculated into 10-day-old specific-pathogen-free chicken embryos (National Poultry Laboratory Animal Resource Center, Harbin Veterinary Research Institute, Chinese Academy of Agriculture Sciences, Harbin, China). After 72 hours of incubation, the allantoic fluid was harvested, and the hemagglutinin (HA) activity was assayed. HA-positive isolates were further subtyped by hemagglutinin inhibition and neuraminidase inhibition assays. Viral RNA was extracted from HA-positive allantoic fluid by using QIAamp Viral RNA Mini Kit (QIAGEN, https://www.qiagen.com), reverse transcribed by using the primer Un12 and subjected to reverse transcription PCR by using the method of the World Health Organization.

Genome Sequencing

The PCR products of 8t fragments of the Ningxia H5N8 isolates were sequenced by using a set of specific sequencing primers previously reported (*1*). The sequence data were compiled by using the SeqMan Program (DNASTAR, https://www.dnastar.com). Thirteen H5N8 influenza viruses were isolated from 6 mallards (*Anas platyrhynchos*), 6 common teals (*A. crecca*), and 1 common pochard (*Aythya ferina*). Nucleotide sequences have been deposited in GISAID (https://www.gisaid.org) under accession nos. EPI_ISL_2815336, EPI_ISL_2815374, EPI_ISL_2820250, EPI_ISL_2820259, EPI_ISL_2820261, EPI_ISL_2820262, EPI_ISL_2820288, EPI_ISL_2820465, EPI_ISL_2820479, EPI_ISL_2820480, EPI_ISL_2820501, EPI_ISL_2820503, and EPI_ISL_2820504.

Phylogenetic Analysis

Homologous sequences of the Ningxia H5N8 isolates were obtained by BLAST search at the GISAID Epiflu databases in early January 2021, and 8 datasets were derived from the top 100 BLASTn hits and the genome of clade 2.3.4.4 H5N8 viruses isolated in 2020. Sequences without full alignment length were excluded. Sequences were aligned by using MAFFT (*2*) implemented in PhyloSuite version 1.2.1 (*3*). The maximum-likelihood tree of each gene was estimated by using IQ-TREE (*4*) under the best-fit substitution model for 1,0000 ultrafast bootstraps (*5*). Best-fit substitution model was selected by using the Bayesian information criterion by ModelFinder (*6*) implemented in PhyloSuite 1.21 (*3*).

For estimation of the time to the most recent common ancestor, Bayesian analysis was performed for all 8 gene segments by using BEAST version 1.10.4. (*7*). The best-fit substitution model was chosen as described above. We specified an uncorrelated lognormal relaxed clock and constant size tree prior for each segment (*8,9*). A Markov

chain Monte Carlo method was used with 50 million chain lengths to draw inference under this model. Three independent runs were combined for analyses to ensure that an adequate effective sample size (200). A maximum clade credibility tree with mean height was generated for each dataset by using TreeAnnotator version 1.10.4 (https://beast.community/treeannotator) after 10% burn-in. The maximum clade credibility trees were visualized by using FigTree version 1.4.4 (http://tree.bio.ed.ac.uk).

Satellite Tracking

On October 15 and 16, 2020, apparently healthy mallards among the sampled birds were chosen for the satellite tracking study. We recorded bodyweight, age (adult or juvenile) and sex for each mallard before equipping them with GPS-GSM (Global Positioning System—Global System for Mobile Communications), solar-powered backpack transmitters. All mallards were released at the capture site instantly after equipping. The transmitters were obtained from Hunan Global Messenger Technology Co. Ltd., https://en.hqxs.net), and the model is HQBG1815S (http://www.hqxs.net/). The transmitters weighed 1.4%–1.5% of the mallards' body mass (average 1,032 g). Location data of the GPS transmitters were acquired from the China Mobile Communication System at 1 location in 2 h intervals by using GSM cards and were reported as latitude, longitude, and location time. The accuracy of the GPS transmitters was categorized into 5 classes: A (± 5 m), B (± 10 m), C (± 20 m), D (± 100 m), and E (± 2,000 m), and the positioning accuracy credibility is 95%. We restricted accuracy to A, B, C, and D for our analysis. We identified the wintering and stopover sites by major clusters of sequential position data, which contrasted with consistent movements and high flight speed (km/hr) during migration. This data enabled identification of the arrival and departure dates at the wintering or stopover sites, and we were able to identify the timing and duration of stopovers and migration flights, as well as the distances between stopovers. If the emitted

signals lost for >1 month, it implied that the transmitter-tagged bird was sick or dead, then the flyway monitoring was terminated.

References

1. Chai H. Molecular epidemiological study on influenza virus in wild birds of Heilongjiang [PhD dissertation]. Harbin (China): Northeast Forestry University; 2012.

2. Katoh K, Standley DM. MAFFT multiple sequence alignment software version 7: improvements in performance and usability. Mol Biol Evol. 2013;30:772–80. PubMed https://doi.org/10.1093/molbev/mst010

3. Zhang D, Gao F, Jakovlić I, Zou H, Zhang J, Li WX, et al. PhyloSuite: an integrated and scalable desktop platform for streamlined molecular sequence data management and evolutionary phylogenetics studies. Mol Ecol Resour. 2020;20:348–55. PubMed https://doi.org/10.1111/1755-0998.13096

4. Nguyen LT, Schmidt HA, von Haeseler A, Minh BQ. IQ-TREE: a fast and effective stochastic algorithm for estimating maximum-likelihood phylogenies. Mol Biol Evol. 2015;32:268–74. PubMed https://doi.org/10.1093/molbev/msu300

5. Minh BQ, Nguyen MA, von Haeseler A. Ultrafast approximation for phylogenetic bootstrap. Mol Biol Evol. 2013;30:1188–95. PubMed https://doi.org/10.1093/molbev/mst024

6. Kalyaanamoorthy S, Minh BQ, Wong TK, von Haeseler A, Jermiin LS. ModelFinder: fast model selection for accurate phylogenetic estimates. Nat Methods. 2017;14:587–9. PubMed https://doi.org/10.1038/nmeth.4285

7. Drummond AJ, Rambaut A. BEAST: Bayesian evolutionary analysis by sampling trees. BMC Evol Biol. 2007;7:214. PubMed https://doi.org/10.1186/1471-2148-7-214

8. Drummond AJ, Ho SY, Phillips MJ, Rambaut A. Relaxed phylogenetics and dating with

confidence. PLoS Biol. 2006;4:e88. PubMed

https://doi.org/10.1371/journal.pbio.0040088

9. Kingman JF. The coalescent. Stochastic Process Appl. 1982;13:235–48.

https://doi.org/10.1016/0304-4149(82)90011-4

Appendix Table 1. Information of the thirteen H5N8 viruses isolated in Ningxia, China, October 2020

GISAID accession no.	Isolate name	Collection date	Clade	Abbreviation
EPI_ISL_2815336	A/common teal/Ningxia/105/2020(H5N8)	2020-Oct-11	2.3.4.4b2	NX-105
EPI_ISL_2815374	A/mallard/Ningxia/175/2020(H5N8)	2020-Oct-15	2.3.4.4b1	NX-175
EPI_ISL_2820250	A/mallard/Ningxia/176/2020(H5N8)	2020-Oct-15	2.3.4.4b1	NX-176
EPI_ISL_2820259	A/common teal/Ningxia/181/2020(H5N8)	2020-Oct-15	2.3.4.4b1	NX-181
EPI_ISL_2820261	A/common teal/Ningxia/189/2020(H5N8)	2020-Oct-15	2.3.4.4b1	NX-189
EPI_ISL_2820262	A/common teal/Ningxia/237/2020(H5N8)	2020-Oct-16	2.3.4.4b1	NX-237
EPI_ISL_2820288	A/mallard/Ningxia/239/2020(H5N8)	2020-Oct-16	2.3.4.4b1	NX-239
EPI_ISL_2820465	A/mallard/Ningxia/241/2020(H5N8)	2020-Oct-16	2.3.4.4b1	NX-241
EPI_ISL_2820479	A/common pochard/Ningxia/243/2020(H5N8)	2020-Oct-16	2.3.4.4b1	NX-243
EPI_ISL_2820480	A/common teal/Ningxia/245/2020(H5N8)	2020-Oct-16	2.3.4.4b1	NX-245
EPI_ISL_2820501	A/mallard/Ningxia/247/2020(H5N8)	2020-Oct-16	2.3.4.4b1	NX-247
EPI_ISL_2820503	A/mallard/Ningxia/249/2020(H5N8)	2020-Oct-16	2.3.4.4b1	NX-249
EPI_ISL_2820504	A/common teal/Ningxia/253/2020(H5N8)	2020-Oct-16	2.3.4.4b1	NX-253

Appendix Table 2. Characteristics of 9 mallards (*Anas platyrhynchos*) we successfully satellite tracked and their migration movements up to May 2021

Bird ID	Sex (Age)*	Weight (g)	Equiping date	AIV test result	Wintering site	Arrival date at wintering site	Departure date at wintering site
NX-166	F (A)	1,010	2020-Oct-15	Negative	Ningxia	Before 2020-Oct-15	2021-Mar-31
NX-167	M (A)	1,115	2020-Oct-15	Negative	Henan	2020-Oct-21	2021-Mar-25
NX-169	M (A)	1,050	2020-Oct-15	Negative	Ningxia	Never left Ningxia	
NX-170	M (A)	925	2020-Oct-15	Negative	Ningxia	Before 2020-Oct-15	2021-Apr-22
NX-173	M (A)	1,100	2020-Oct-15	Negative	Ningxia	Before 2020-Oct-15	2021-Apr-7
NX-174	M (A)	1,000	2020-Oct-15	Negative	Ningxia	Never left Ningxia	
NX-175	F (A)	1,060	2020-Oct-15	H5N8	Gansu	2020-Oct-16	
NX-176	M (A)	1,030	2020-Oct-16	H5N8	Ningxia	Never left Ningxia	
NX-231	F (A)	995	2020-Oct-16	Negative	Sichuan	2020-Dec-24	2021-Mar-24

*A, adult; AIV, avian influenza virus.

Appendix Table 3. Information for clade 2.3.4.4b1 isolates in this study

Date	Location	Isolate name	Isolate ID
2020-Oct-21	South Korea	A/Mandarin duck/Korea/H242/2020	EPI_ISL_631824
2020-Oct-24	South Korea	A/Mandarin duck/Korea/K20–551–4/2020	EPI_ISL_666687
2020-Oct-24	Japan	A/northern pintail/Hokkaido/M13/2020	EPI_ISL_697771
2020-Nov-09	Japan	A/environment/Kagoshima/KU-ngr-J2/2020(H5N8)	EPI_ISL_682297
2019-Dec-30	Poland	A/turkey/Poland/23/2019	EPI_ISL_402134
2020-Jan-01	Poland	A/laying_hen/Poland/002/2020	EPI_ISL_525439
2020-Jan-02	Poland	A/chicken/Poland/003/2020	EPI_ISL_525440
2020-Jan-02	Poland	A/chicken/Poland/004/2020	EPI_ISL_525441
2020-Jan-06	Poland	A/hawk/Poland/003/2020	EPI_ISL_405813
2020-Jan-09	Poland	A/turkey/Poland/027/2020	EPI_ISL_525442
2020-Jan-12	Poland	A/domestic_goose/Poland/028/2020	EPI_ISL_525443
2020-Jan-17	Poland	A/chicken/Poland/054/2020	EPI_ISL_525444
2020-Jan-25	Poland	A/turkey/Poland/079/2020	EPI_ISL_525445
2020-Jan-27	Poland	A/laying_hen/Poland/095/2020	EPI_ISL_525446
2020-Jan-28	Poland	A/turkey/Poland/096/2020	EPI_ISL_525447
2020-Feb-20	Poland	A/domestic_duck/Poland/219/2020	EPI_ISL_525449
2020-Feb-20	Poland	A/domestic_duck/Poland/221/2020	EPI_ISL_525450
2020-Feb-21	Poland	A/domestic_duck/Poland/222/2020	EPI_ISL_525451
2020-Mar-01	Poland	A/domestic_goose/Poland/274/2020	EPI_ISL_525462
2020-Jan-16	Germany	A/white-fronted goose/Germany-BB/AI00018/2020(H5N8)	EPI_ISL_404993
2020-Feb-06	Germany	A/chicken/Germany-BW/AI00049/2020	EPI_ISL_410291
2020-Mar-12	Germany	A/chicken/Germany-SN/AI00276/2020	EPI_ISL_415197
2020-Mar-20	Germany	A/buzzard/Germany-SN/AI00285/2020	EPI_ISL_417414
2020-Mar-20	Germany	A/turkey/Germany-NI/AI00334/2020	EPI_ISL_417415
2020-Mar-26	Germany	A/steamer duck/Germany-SN/AI00346/2020	EPI_ISL_419312
2020-Mar-27	Germany	A/turkey/Germany-ST/AI00352/2020	EPI_ISL_419314
2020-Jan-17	Czech Republic	A/chicken/Czech Republic/1175–1/2020	EPI_ISL_405391
2020-Feb-17	Czech Republic	A/turkey/Czech Republic/3071/2020	EPI_ISL_418266
2020-Jan-09	Hungary	A/turkey/Hungary/1020_20VIR749–1/2020	EPI_ISL_419220
2020-Mar-25	Hungary	A/Duck/Hungary/14788/2020	EPI_ISL_780096
2020-Mar-26	Hungary	A/Goose/Hungary/15267/2020	EPI_ISL_796011

Appendix Table 4. Time of the most recent common ancestor of selected node that contained each gene segment of viruses associated with H5N8 viruses isolated in Ningxia, China, October 2020*.

Segment	Node†	tMRCA	95% HPD		Posterior value
			Earliest date	Latest date	
PB2	1	2020 Sep.	2020 Aug.	2020 Sep.	0.9873
	2	2020 Jul.	2020 May.	2020 Sep.	1
	3	2020 Aug.	2020 Jul.	2020 Oct.	0.9989
PB1	1	2020 Jul.	2020 Apr.	2020 Sep.	1
	2	2020 Jul.	2020 May.	2020 Aug.	0.2388
PA	1	2020 Aug.	2020 Jul.	2020 Sep.	1
	2	2020 May.	2020 Feb.	2020 Aug.	1
	3	2020 Aug.	2020 Jul.	2020 Sep.	0.4015
HA	1	2020 Sep.	2020 Jul.	2020 Sep.	1
	2	2020 May.	2020 Feb.	2020 Aug.	1
	3	2020 Jun.	2020 Apr.	2020 Aug.	0.4552
NP	1	2020 Jun.	2020 Mar.	2020 Aug.	1
	2	2020 Aug.	2020 Jul.	2020 Oct.	1
NA	1	2020 Aug.	2020 Jun.	2020 Sep.	0.9702
	2	2020 Jun.	2020 Feb.	2020 Sep.	1
	3	2020 Aug.	2020 Jun.	2020 Oct.	0.5622
M	1	2020 Sep.	2020 Aug.	2020 Oct.	0.9999
	2	2020 Aug.	2020 May.	2020 Sep.	1
	3	2020 Oct.	2020 Aug.	2020 Oct.	0.9767
NS	1	2020 Sep.	2020 Aug.	2020 Oct.	1
	2	2020 Jul.	2020 Apr.	2020 Sep.	1
	3	2020 Sep.	2020 Aug.	2020 Oct.	0.9613

*HPD, highest posterior density; PB2, polymerase basic 2; PB1, polymerase basic 1; PA, polymerase acidic; HA, hemagglutinin; NP, nucleoprotein; M, matrix; NS, nonstructural; tMRCA, time of the most recent common ancestor.

†Nodes marked in the maximum clade credibility phylogenetic trees (Appendix Figure 2).

Appendix Table 5. Molecular characterization of H5N8 viruses isolated in Ningxia, October 2020, and the H5N8 virus that infected humans in Russia, December 2020*

Protein	Position	Ningxia b1 isolates	Ningxia b2 isolate	A/Astrakhan/3212/2020(H5N8)
HA	S133A	+	+	+
(H5 numbering)†	T156A	+	+	+
	T188I	-	+	-
	V210I	-	+	-
	Q222L	-	-	-
	G224S	-	-	-
PB2‡	Q591K	-	-	-
	E627K	-	-	-
	D701N	-	-	-
M1§	N30D	+	+	+
	I43M	+	+	+
	T215A	+	+	+
NS§	P42S	+	+	+
	80–84 deletion	NO	NO	NO
	L98F	+	+	+
	I101M	+	+	+

*HA, hemagglutinin; PB2, polymerase basic 2; M, matrix; NS, nonstructural; Ningxia b1 isolates, the twelve clade 2.3.4.4b1 H5N8 viruses isolated in Ningxia, October 2020; Ningxia b2 isolate, A/common teal/Ningxia/105/2020(H5N8), the clade 2.3.4.4b2 H5N8 virus isolated in Ningxia, October 2020; +, mutation; –, no mutation.

†S133A, T156A, T188I, V210I, Q222L, and G224S mutations in HA have been associated with increased binding to human-like receptor (α-2–6 sialic acid).

‡Q591K, E627K, and D701N mutations have been associated with increased adaptation of avian influenza virus in mammalian host.

§N30D, I43M, T215A, P42S, 80–84 deletion, L98F, and I101M mutations have been associated with increased virulence in mice.
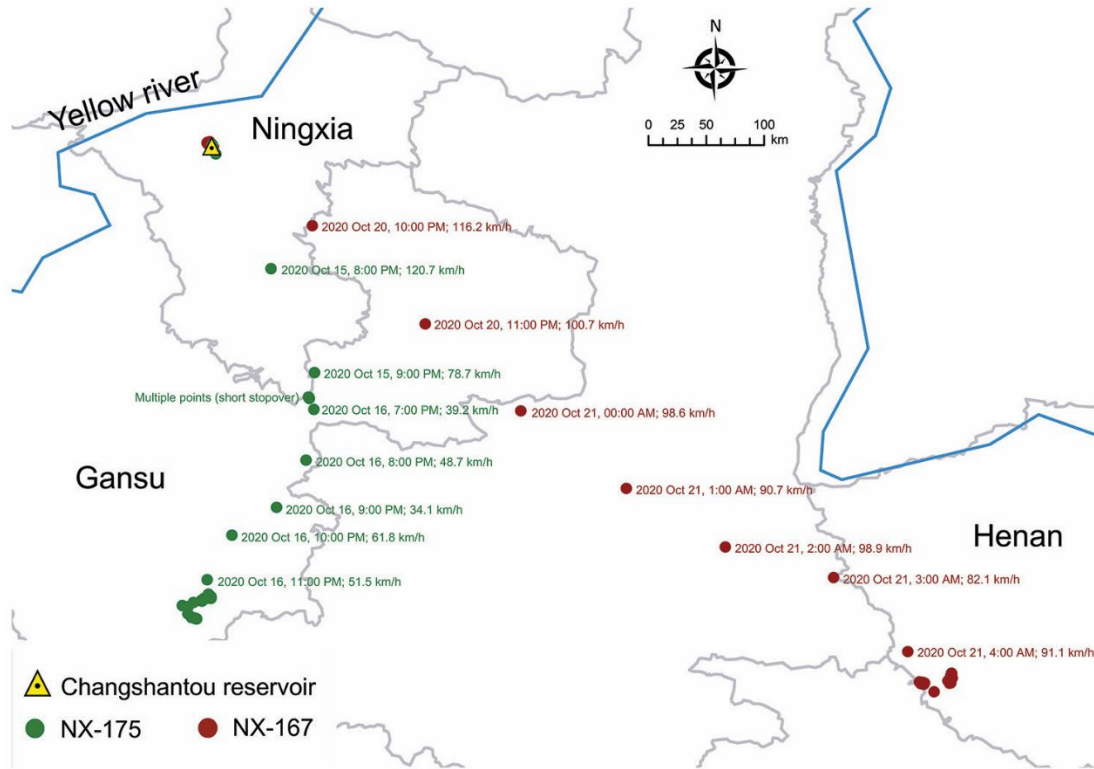
Appendix Figure 1. During October 15–30, 2020, movements of 2 successfully satellite-tracked mallards (*Anas platyrhynchos*). Time and flight speed of every moving point during the migration of the 2 mallards is displayed. The sampling site (Changshantou Reservoir) is indicated.
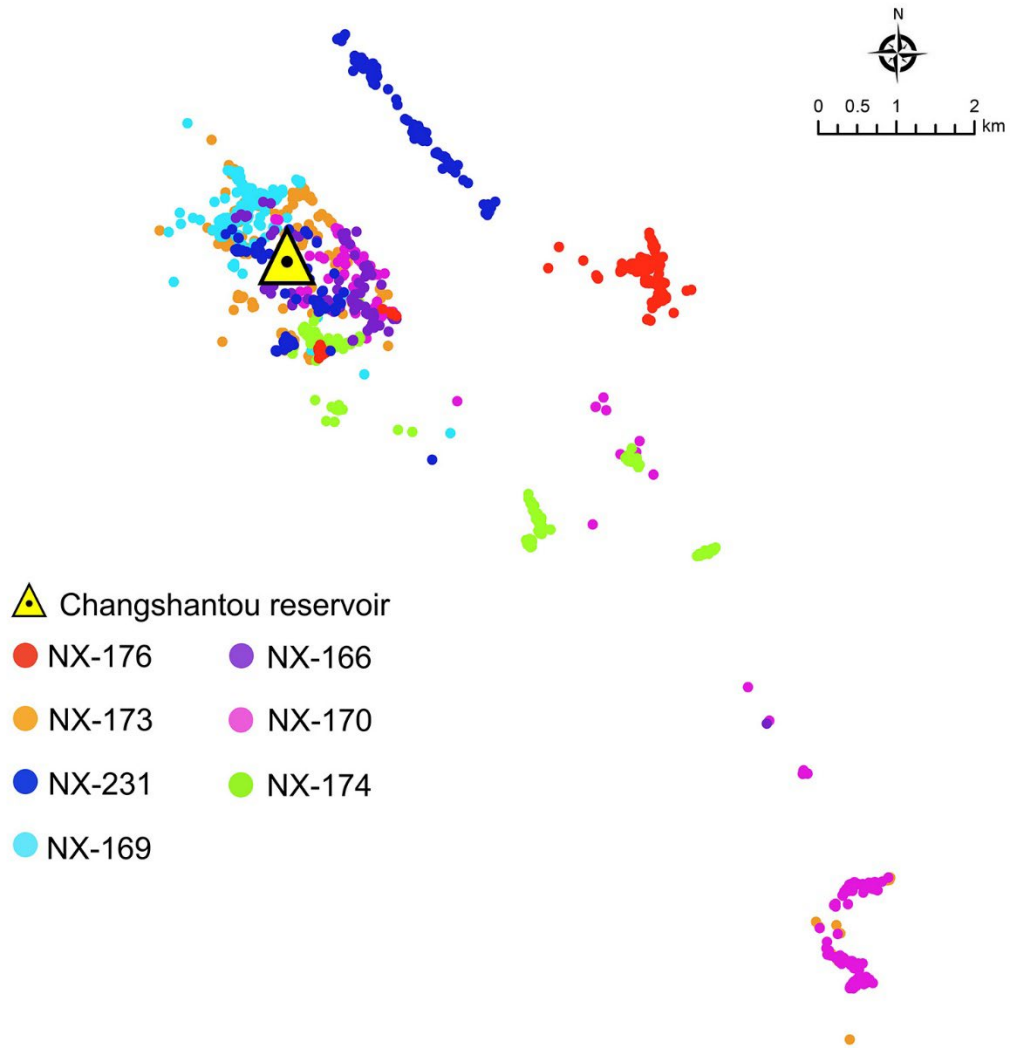
Appendix Figure 2. During October 15–30, 2020, movements of 7 successfully satellite-tracked mallards. Movements are represented by different colors. The sampling site at Changshantou Reservoir is indicated.
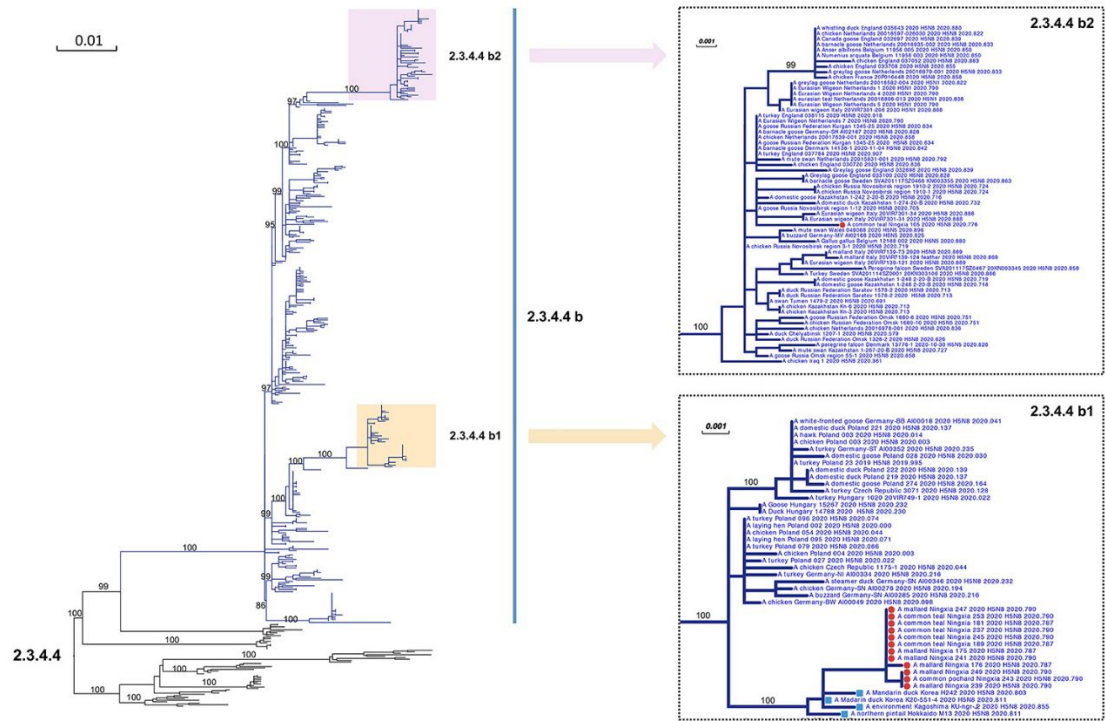
Appendix Figure 3. Maximum-likelihood phylogenetic trees for hemagglutinin genes of avian influenza A(H5N8) viruses isolated in Ningxia, China, 2020, and comparison with clade 2.3.4.4 reference isolates. Dark blue lines indicate viruses that belonged to clade 2.3.4.4b, and black lines indicate viruses that belonged to clade 2.3.4.4a, c–h. Subtrees marked with orange and purple backgrounds indicate subclade 2.3.4.4b1 and subclade 2.3.4.4b2, respectively. The 2 subtrees indicated in the 2 boxes on the right show our Ningxia H5N8 isolates (red circles) and H5N8 viruses isolated from South Korea and Japan during October and November 2020 (blue squares). UFBoot support values of the major branch are indicated. Numbers along branches are bootstrap values. Scale bars indicate nucleotide substitutions per site.

A

0.01
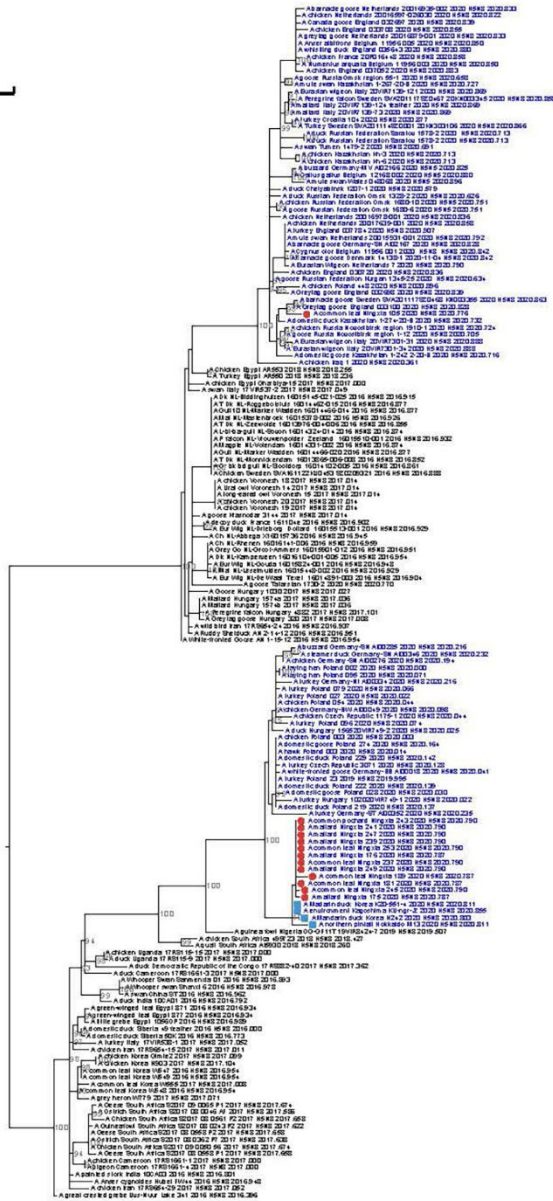
2.3.4.4b2-like

2.3.4.4b1-like

B

0.01

2.3.4.4b2-like

2.3.4.4b1-like

C

2.3.4.4b2-like

2.3.4.4b1-like

0.01

D

0.01

2.3.4.4b2

2.3.4.4b1

2.3.4.4b

E

0.01
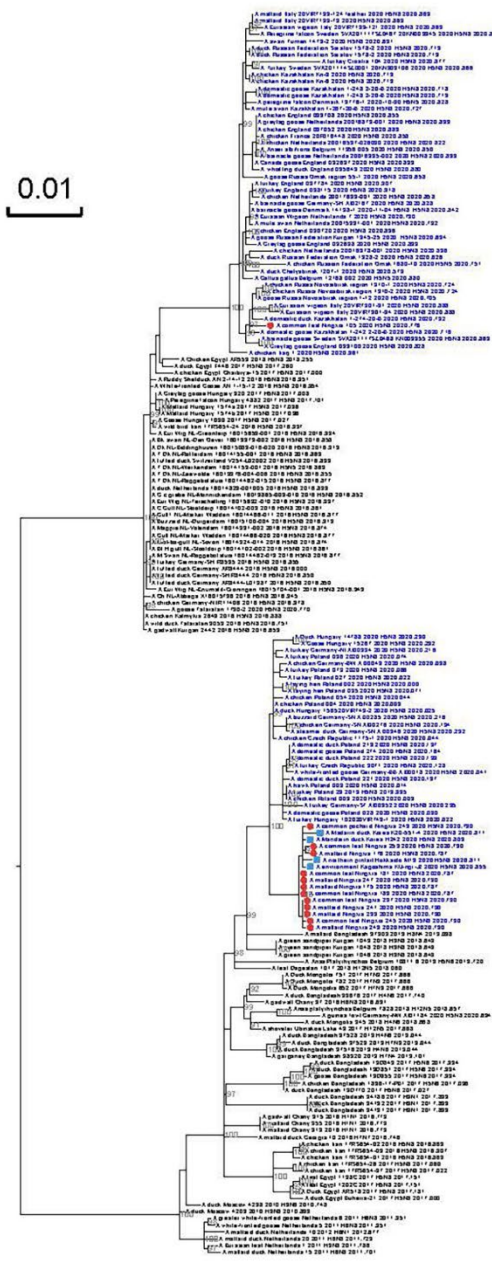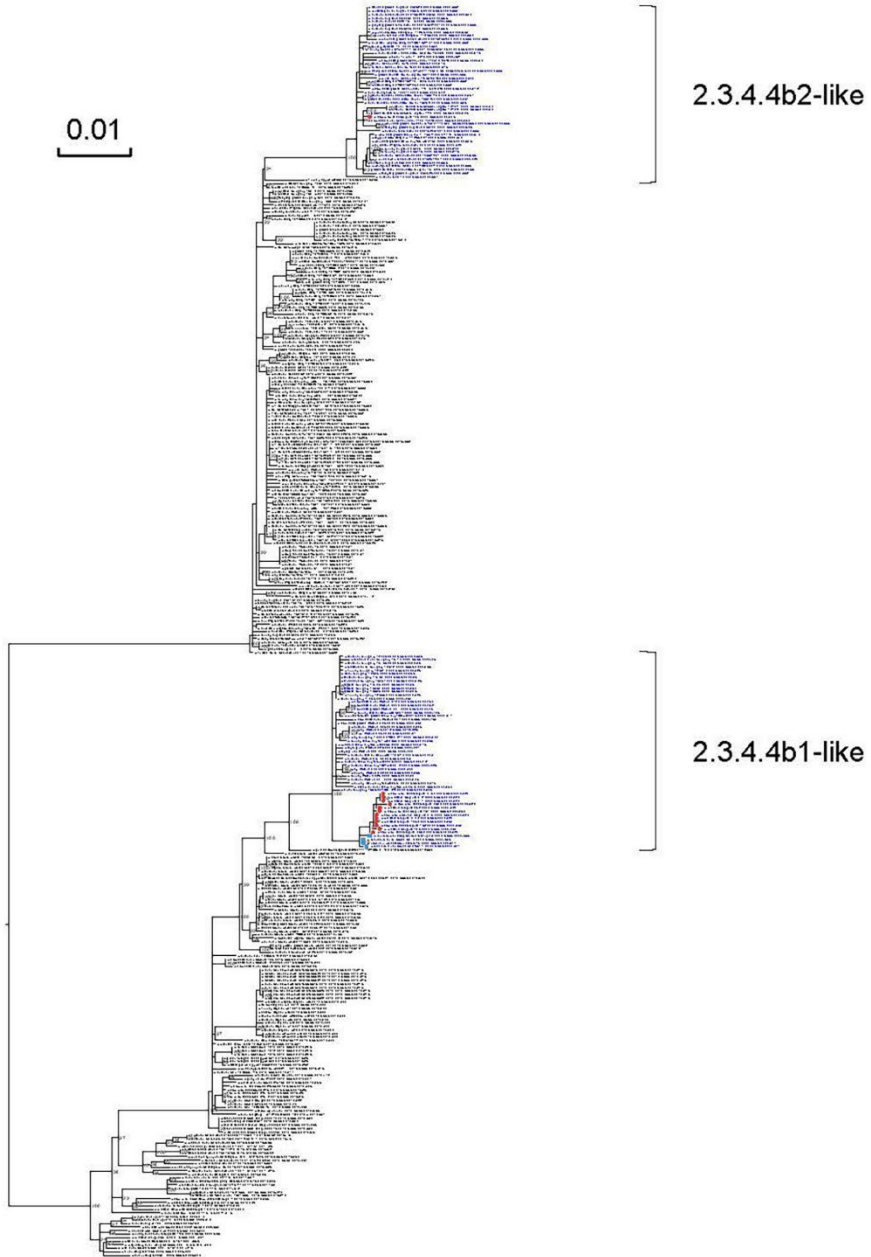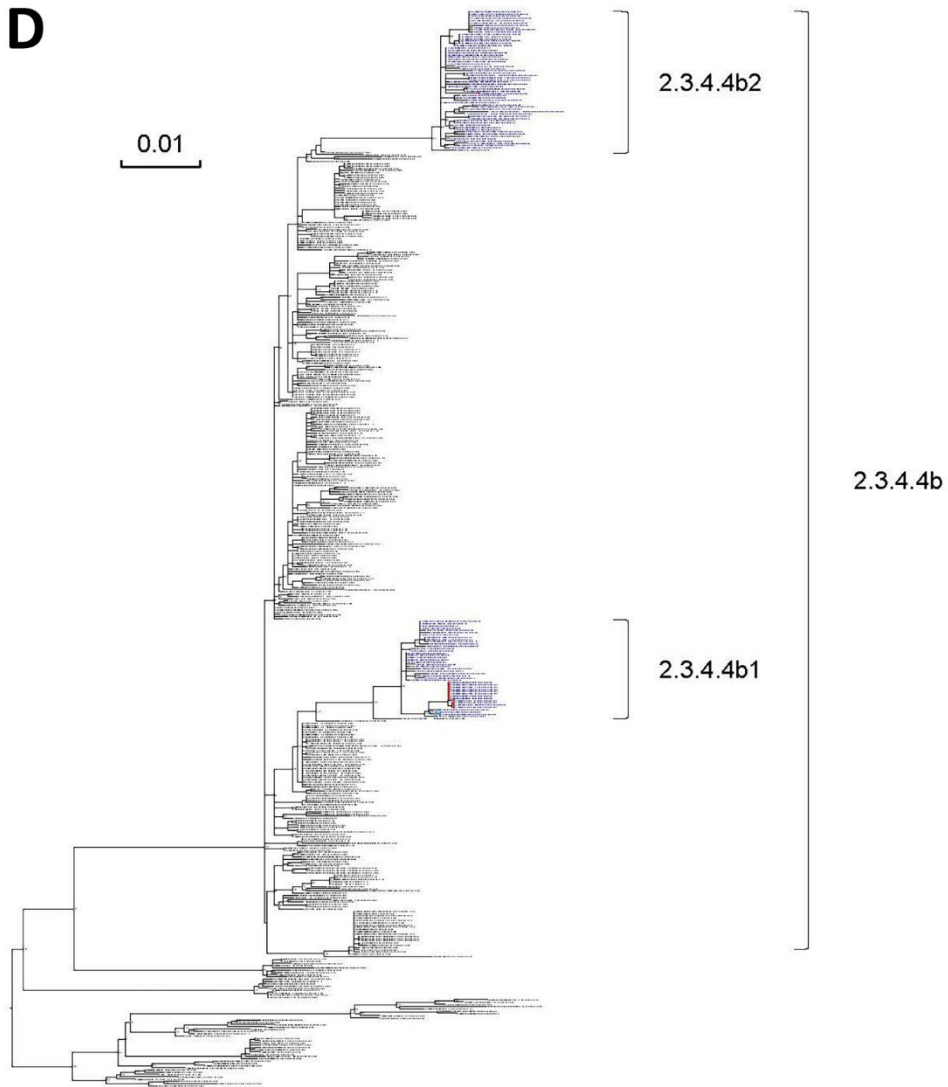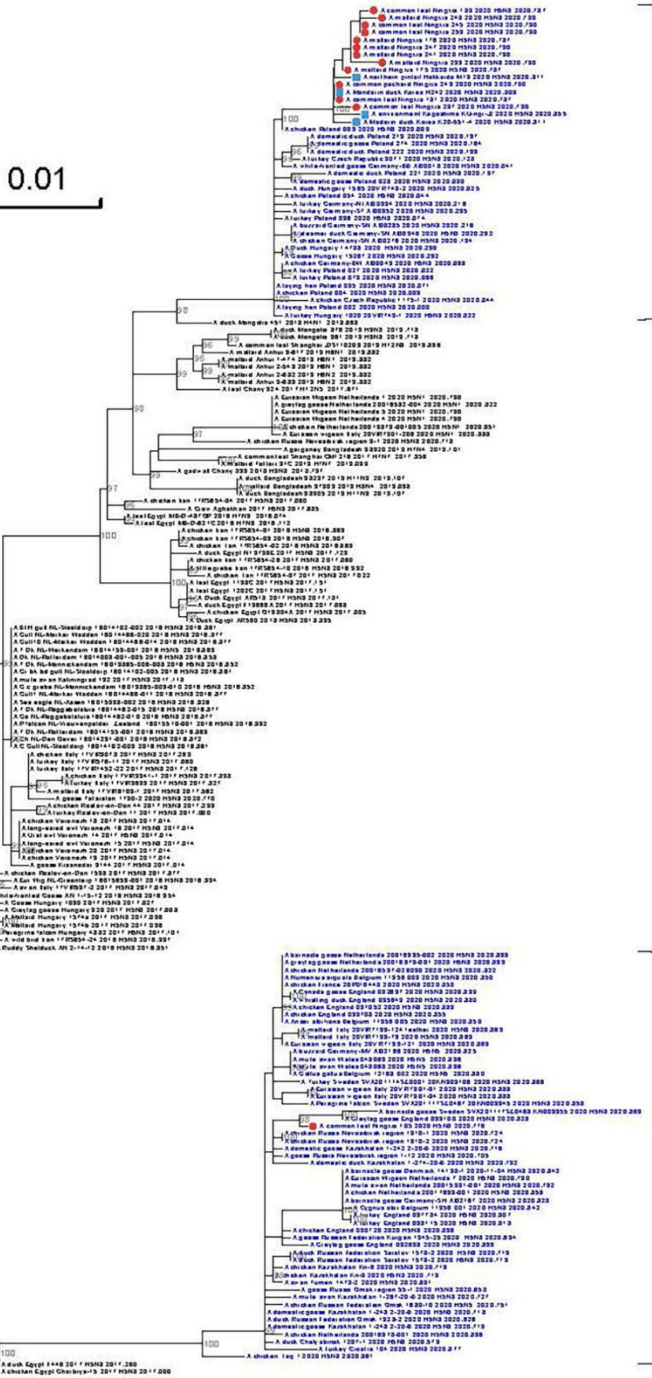
2.3.4.4b1-like

2.3.4.4b2-like

F

0.01
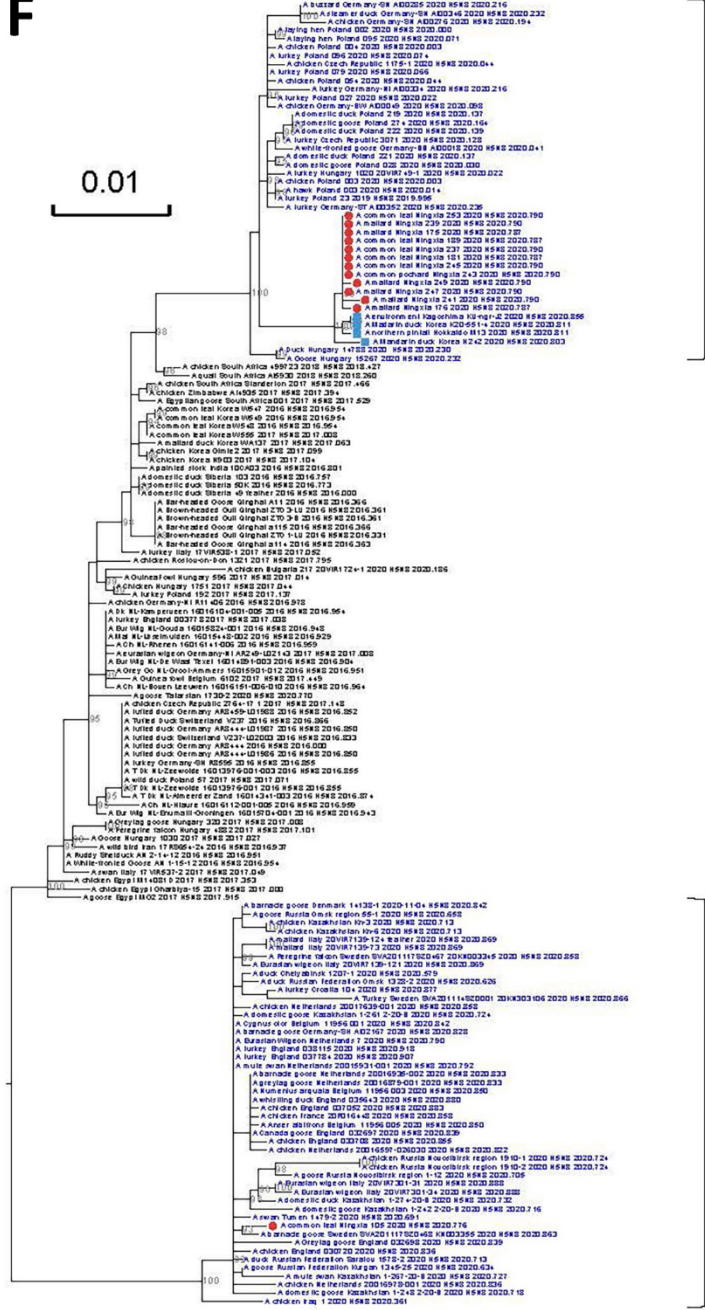
2.3.4.4b1-like

2.3.4.4b2-like

G

0.001
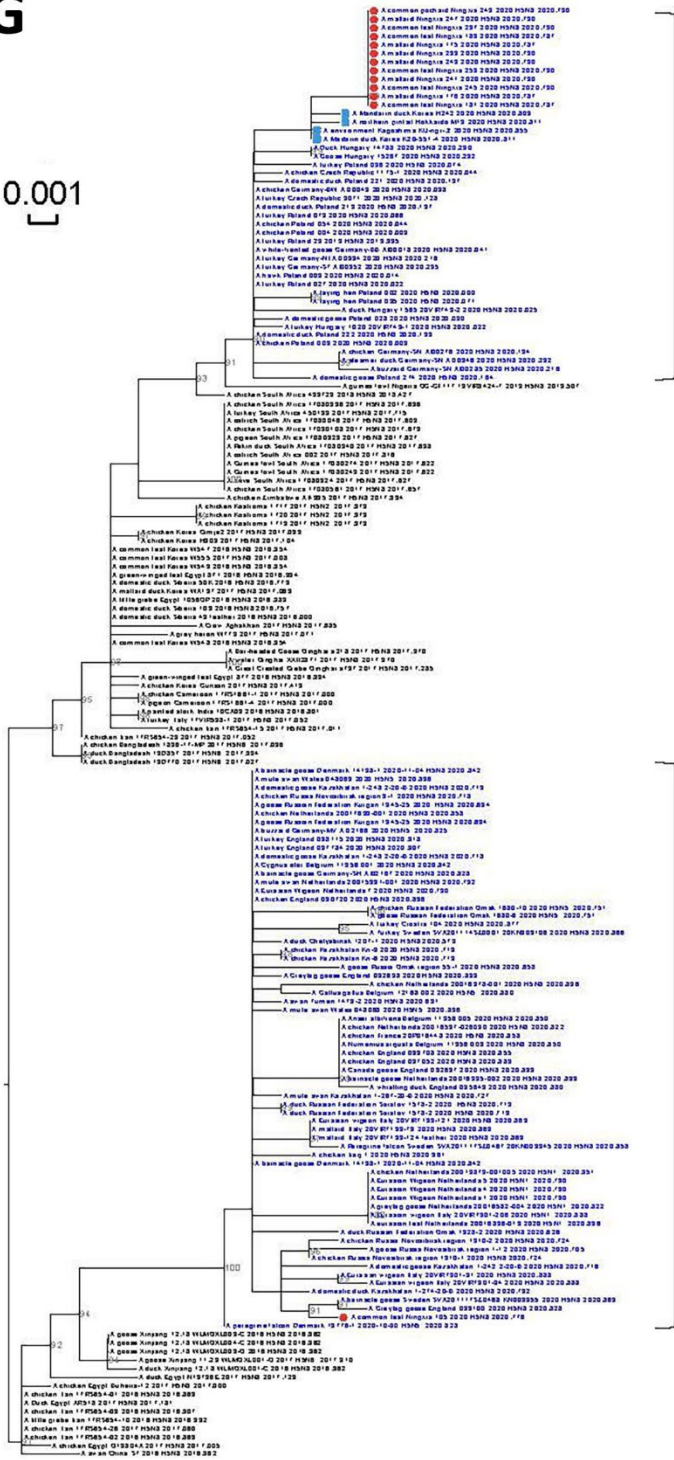
2.3.4.4b1-like
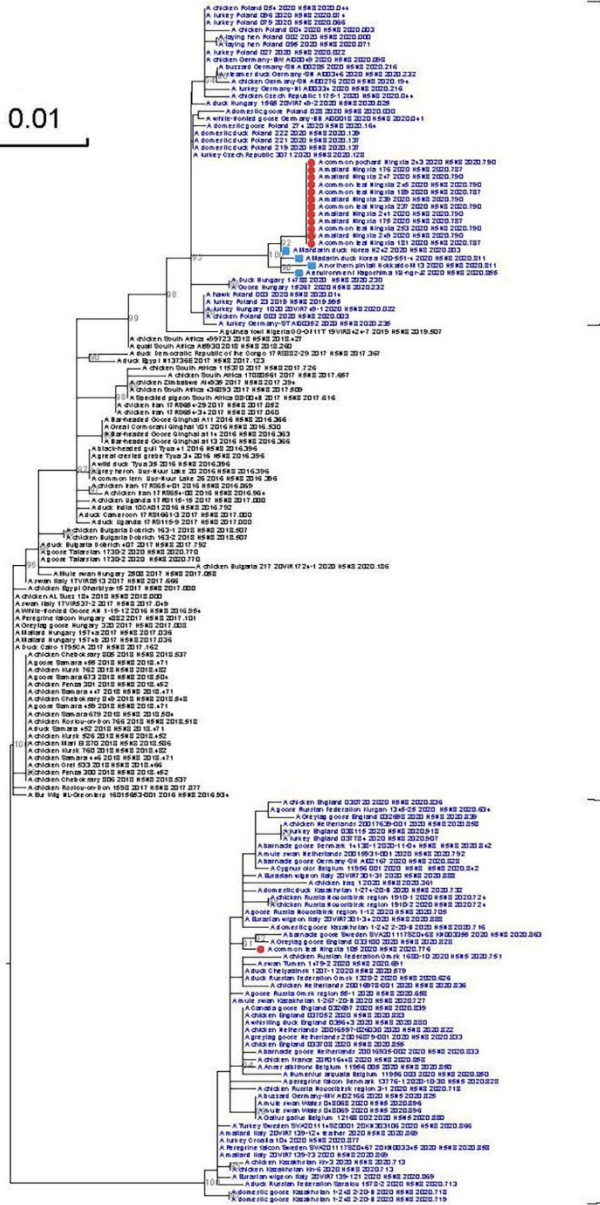
2.3.4.4b2-like

Appendix Figure 4. Maximum-likelihood phylogenetic trees. Our Ningxia H5N8 isolates are marked with red circles, the H5N8 viruses from South Korea and Japan isolated in October and November 2020 are marked with blue squares, and the clade 2.3.4.4b viruses isolated in 2020 are shown in blue. UFBoot support values >90 are shown. A) polymerase basic 2; B) polymerase basic 1; C) polymerase acidic; D) hemagglutinin; E) nucleoprotein; F) neuraminidase; G) matrix; H) nonstructural. Values along branches are bootstrap values. Scale bars indicate nucleotide substitutions per site.

A

C

E

F

G
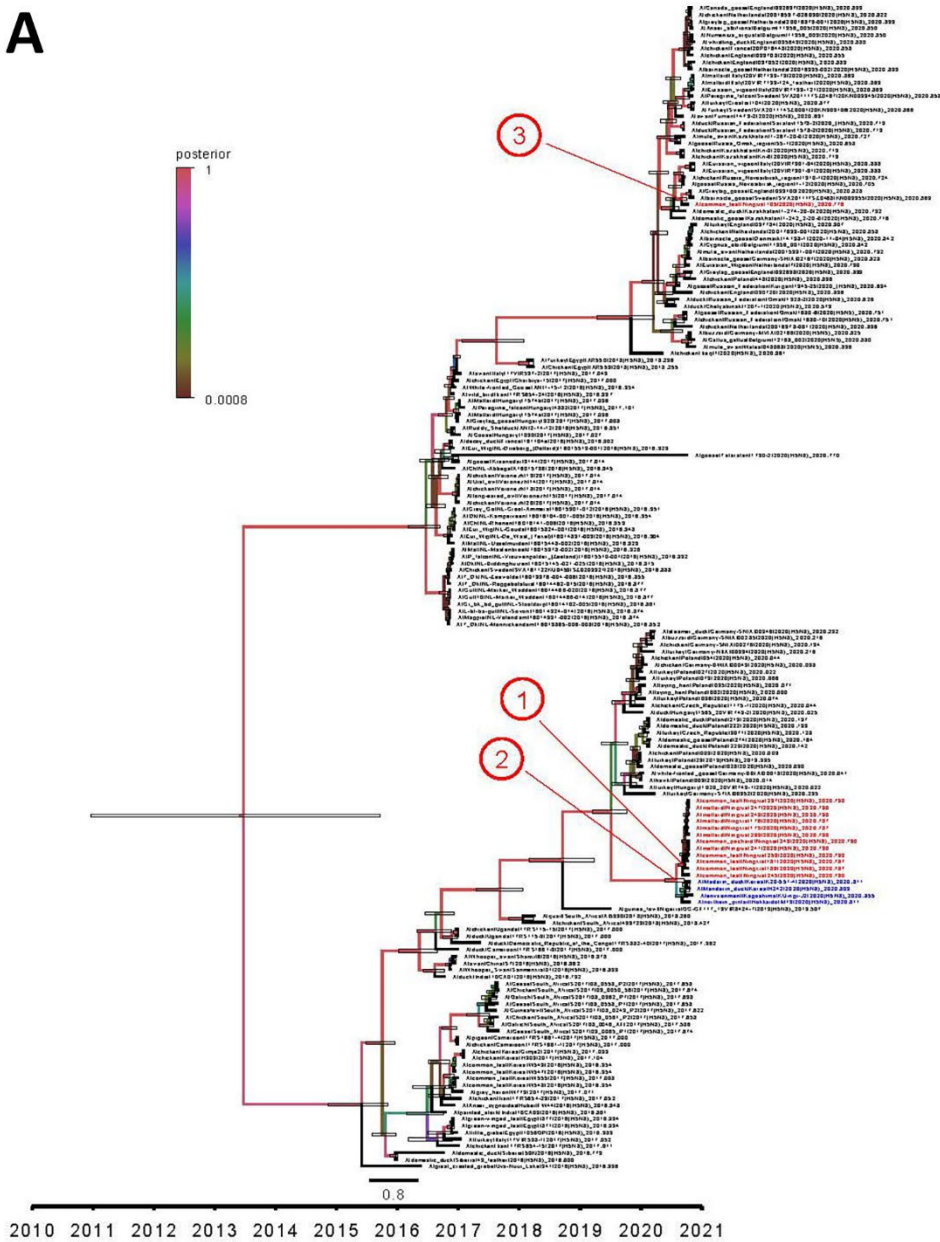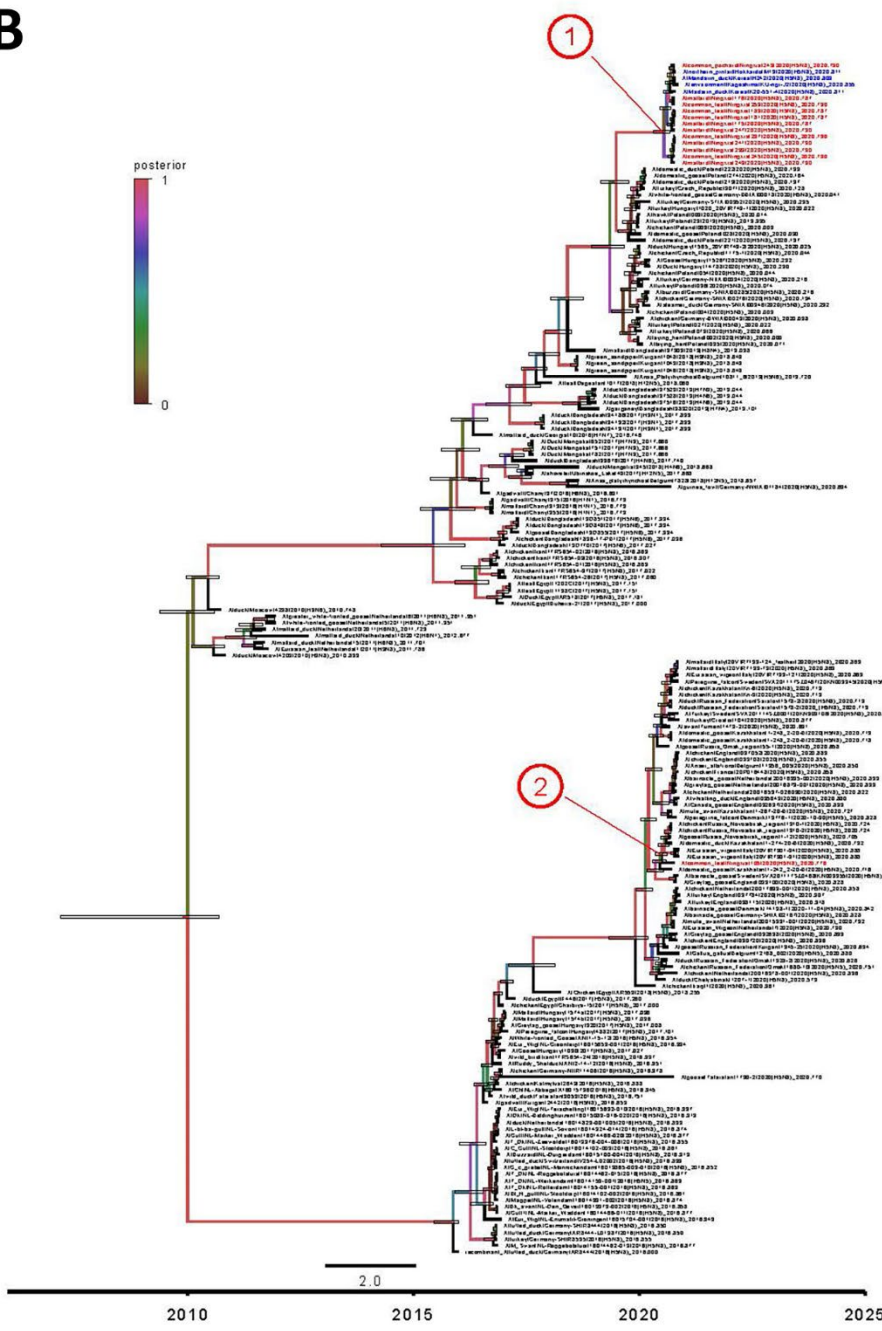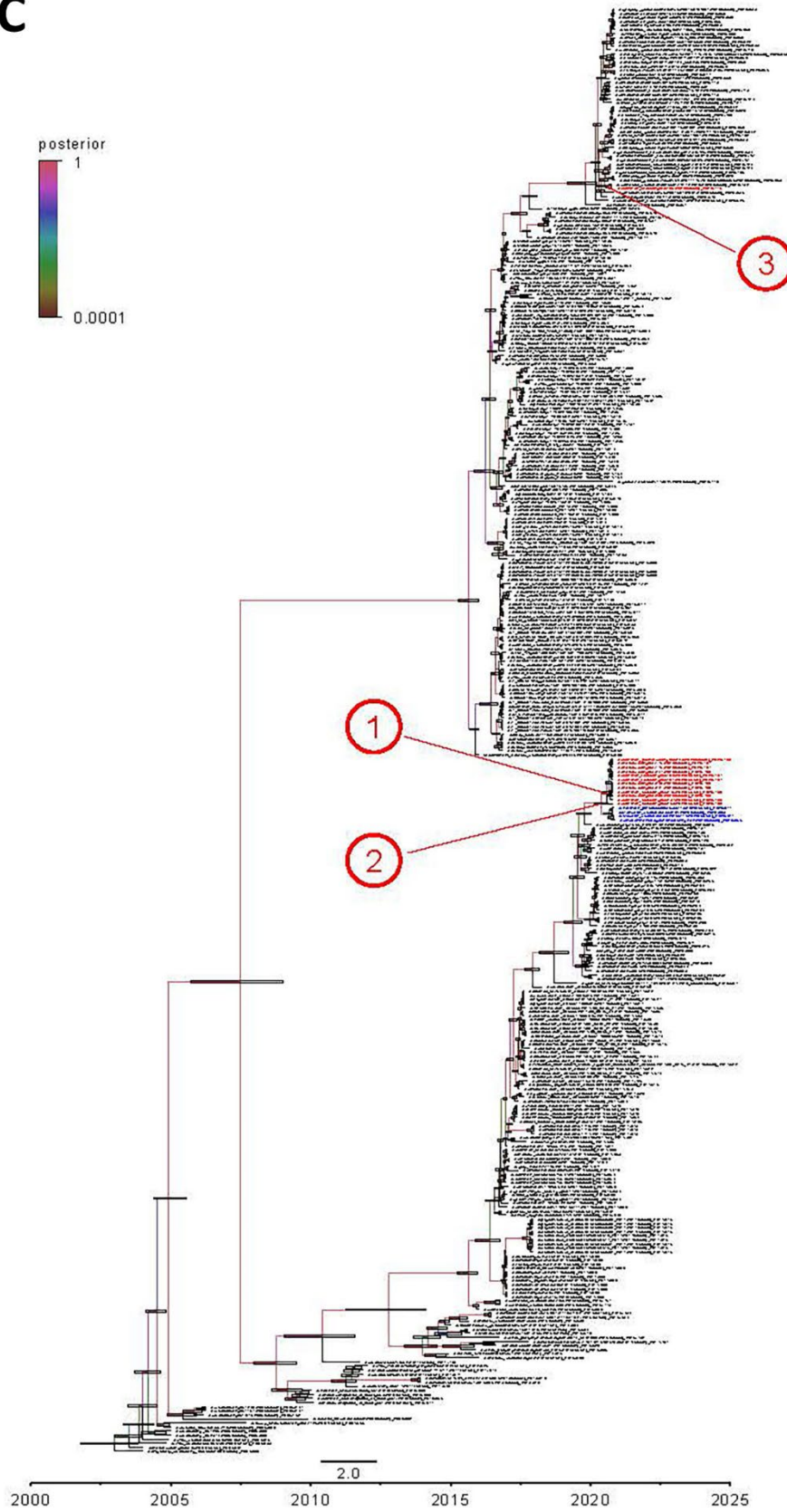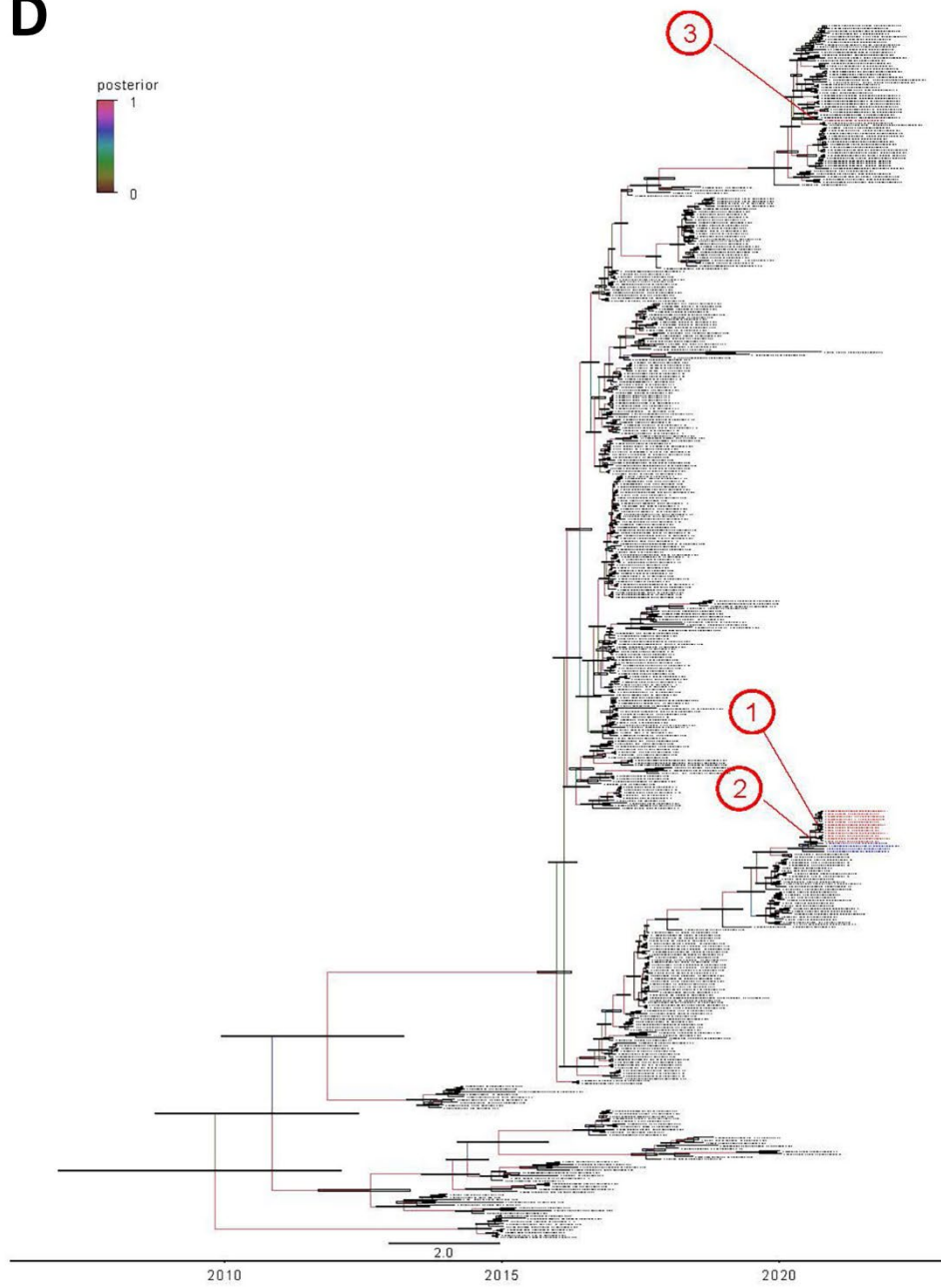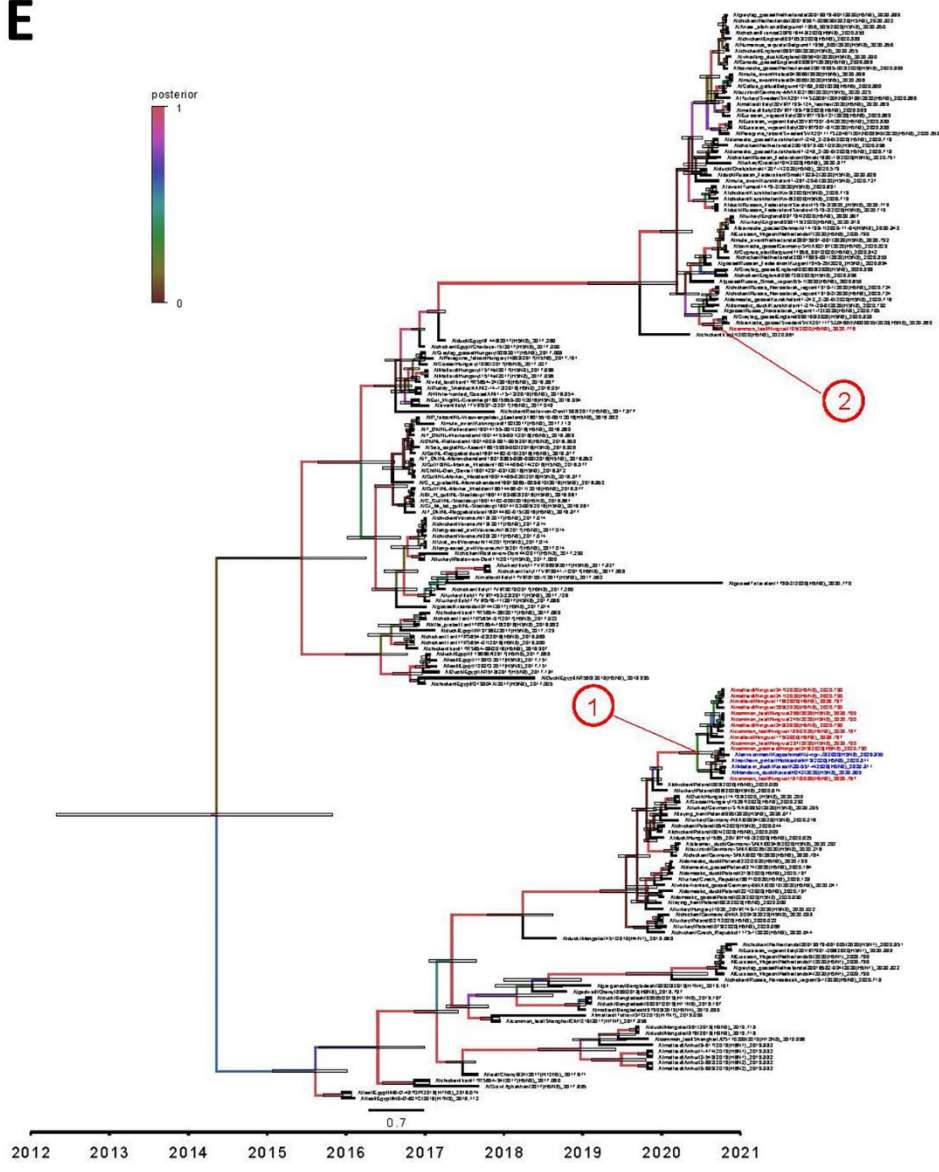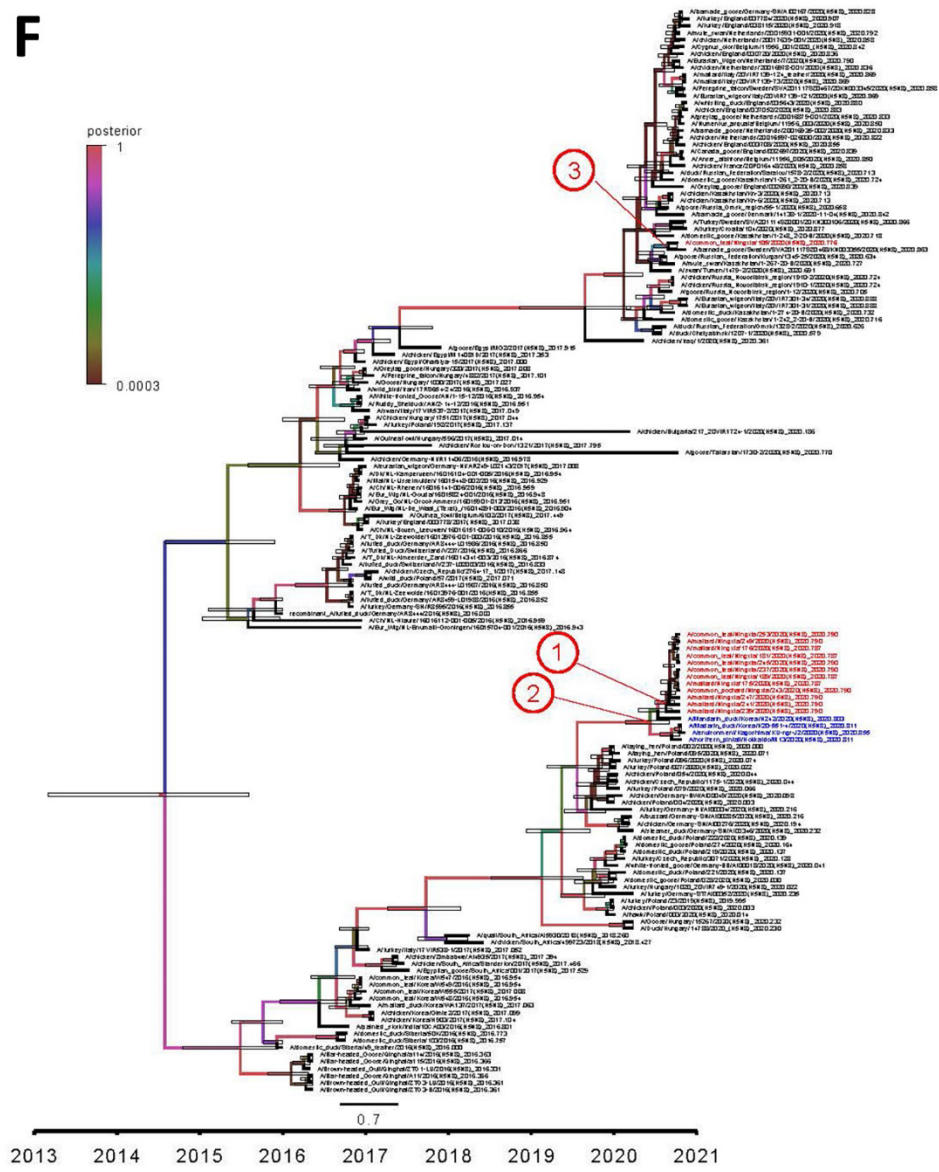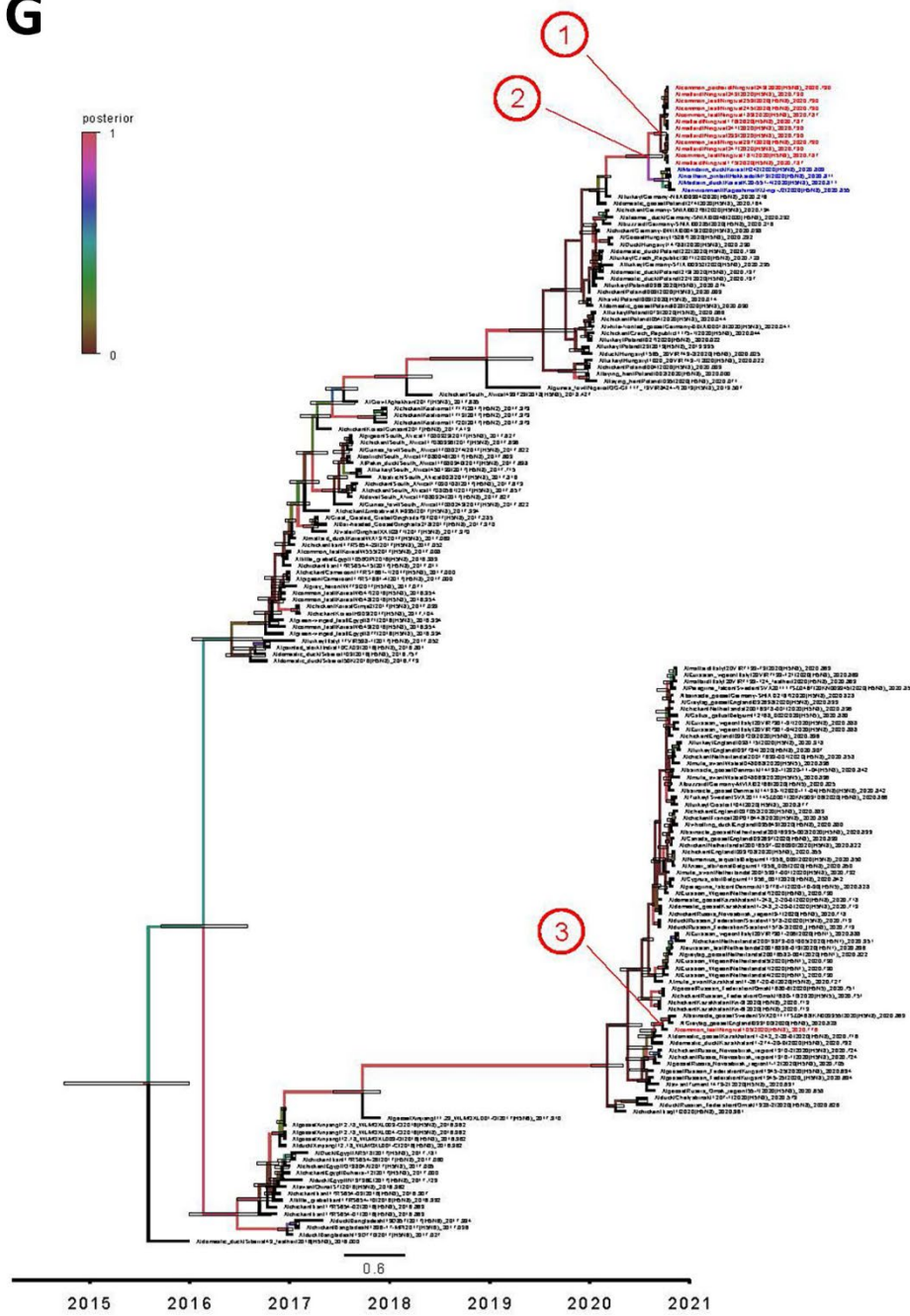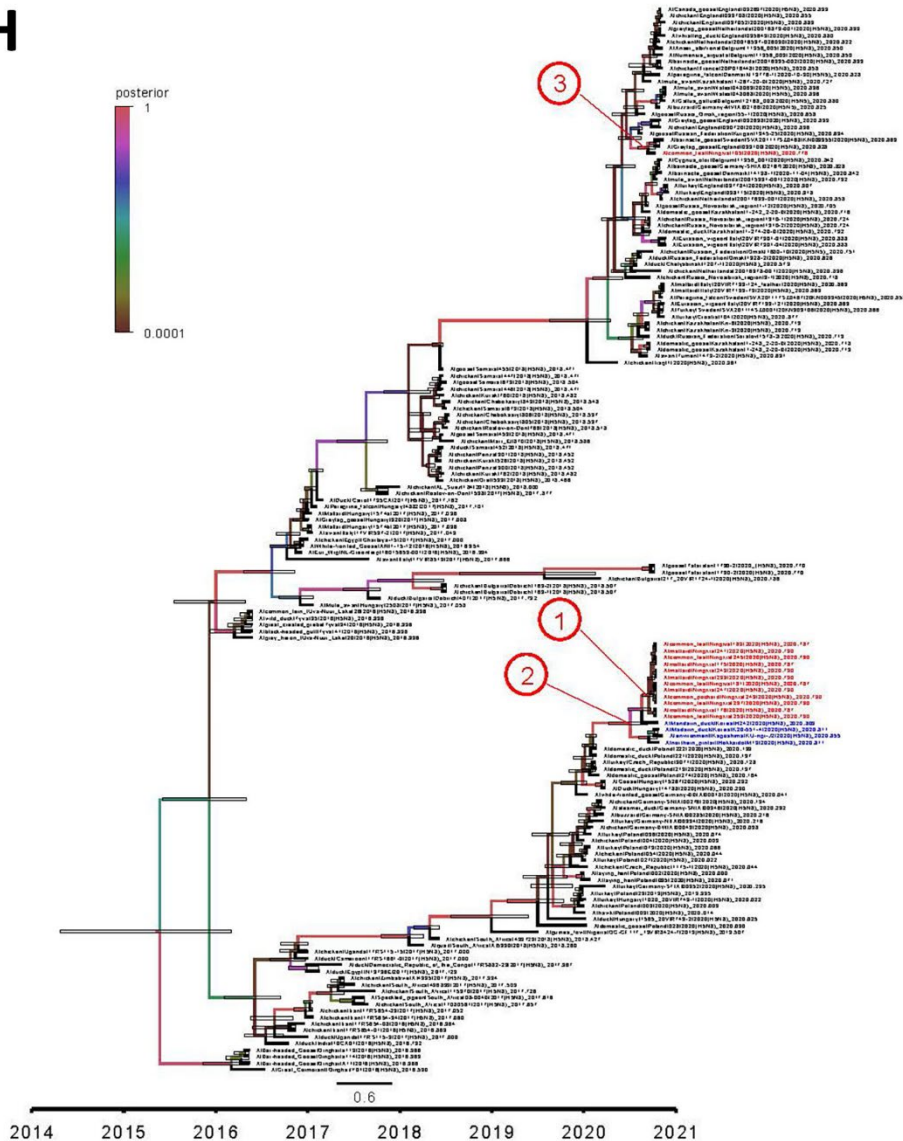
Appendix Figure 5. Maximum clade credibility phylogenetic trees (years on the horizontal axis) of each gene segment of the viruses associated with the H5N8 viruses isolated in Ningxia, October 2020. The Ningxia H5N8 isolates are shown in red, and the H5N8 viruses isolated in South Korea and Japan during October and November 2020 are shown in blue. The horizontal bars indicate the 95% highest posterior density (HPD) intervals of the most recent common ancestor. A) polymerase basic 2; B) polymerase basic 1; C) polymerase acidic; D) hemagglutinin; E) nucleoprotein; F) neuraminidase; G) matrix; H) nonstructural. Values along branches are bootstrap values. Scale bars indicate nucleotide substitutions per site.